

V.Y. Valyaev, O.A. Sapozhnikov

**RADIATION OF WIDEBAND PULSES BY THICK LITHIUM NIOBATE TRANSDUCER:
NUMERICAL SIMULATION**

M.V. Lomonosov Moscow State University,
Faculty of Physics, Department of Acoustics
Leninskie Gory, Moscow 119992, Russia
Tel./Fax: (495) 939-2952
E-mail: oleg@acs366.phys.msu.ru

Based of the finite differences method, numerical algorithm was developed and program was written to describe elastic and electrical processes in cylindrical lithium niobate transducer in the presence of metal back load, liquid frontal load and fixing along the edges. Parameters of signal radiated to liquid were analyzed depending on parameters of case and exciting electrical signal. The possibility of construction of etalon broadband transducer to calibrate hydrophones on basis of thick lithium niobate piezocrystal was investigated.

Introduction

Calibration of broadband hydrophones of megahertz frequency range is important direction of research of applications of ultrasound in different fields, in particular in medical diagnostics and therapy. Such characteristics as sensitivity of sensor and angular reception diagram expect measurement of hydrophone response to a plane wave falling on it. Therefore, construction of calibrated wideband transducers of plane waves is an actual problem. In this work we investigated a possibility suggested in paper [1] of construction of etalon broadband transducer on the basis of a thick lithium niobate piezocrystal. Use of the thick active element is caused by the fact that for the broadband calibration it is required to radiate not only high frequencies, but also low ones: use of thin plates leads to narrow spectrum of radiated signal because of reflections in plate. Cheaper material for active element is piezoceramics, but its grainy structure leads to uncontrollable distortions of signal waveform; moreover, here the wave cease to be plane. Another drawback of the piezoceramics is that their characteristics are usually known with low precision and can significantly vary in time. Monocrystals are devoid of mentioned drawbacks but they are less effective. As it is known lithium niobate is one of the few monocrystals whose effectiveness just insignificantly yields to piezoceramics.

Etalon wave radiated by thick transducer is not plane even in case of an ideal crystal. The reason for this are edge effects which lead to distortions of both electric field and field of mechanical stresses. To decrease them it is required right choice of sizes of different elements of transducer. Analytical accounting of edge effects is practically impossible. In this work numerical algorithm is developed which allows to solve this problem.

Transducer design

Scheme of investigated transducer is presented on Fig. 1. Core of the transducer is cylindrical crystal of lithium niobate (1), z-cut. Excitation voltage $U(t)$ is supplied to a copper backing (2), the case and the radiating surface of the piezoelement are grounded. Signal is radiated to water (6). Air (4) is replaced with vacuum. In addition, auxiliary dielectric ring (5) was introduced, which, as computing showed, allowed to smooth nonuniformities of electric field on the edges of crystal. In numerical simulation elastic stresses were computed only in part of case marked black on Fig. 1. Region filled with water was clipped along the same radius. Surface of

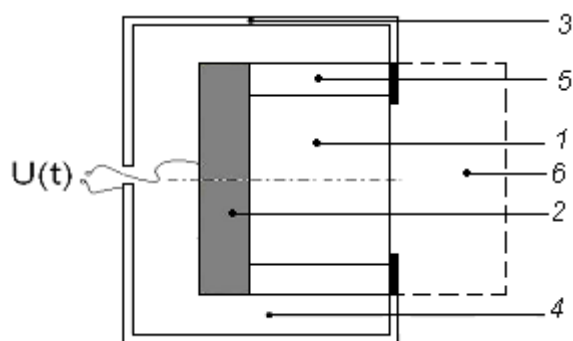


Fig. 1. Scheme of transducer. 1 – lithium niobate crystal; 2 – metal back load; 3 – metal case; 4 – air; 5 – dielectric ring; 6 – water.

clipping of case and water was treated as a pressure release. Due to absence of interaction of elastic and electric fields in mentioned elements this simplification did not affect transient response of transducer in some initial time interval we are interested in. In numerical simulation exciting voltage $U(t)$ considered to be given, i.e. inverse influence of burden to source was not accounted. Reaction of system to exciting signal in the form of "step" $U(t) \sim \text{th}(t/t_0)$, where t_0 is width of transitional front, was regarded.

Electrostatic field analysis

In the first stage of the work it the nonuniformity of electrical static field depending on parameters of case of transducer was examined. For computing was used the package FEMlab 3.1. Piezocrystal of lithium niobate was considered as a single-axis anisotropic dielectric medium, for which diagonal components of permittivity tensor in main axes are: $\varepsilon_{rr} = \varepsilon_{\theta\theta} = \varepsilon_0 \cdot 84.6$, $\varepsilon_{zz} = \varepsilon_0 \cdot 28.6$, where $\varepsilon_0 = 8.85 \cdot 10^{-12}$ F/m, (r, θ, z) - cylindrical coordinates with axis $0z$ being coincident with the axis of the transducer. Thanks to the axial symmetry of the examined device, the problem is two dimensional, because dependence of considered parameters on polar angle θ is missed.

As a result of computing it was found that for the fixed thickness of the crystal, the nonuniformity of the electrical field mostly depends on width of the air gap between side surface of the crystal and the metal case; moreover, there is an optimal value of this parameter to balance between the demands of minimizing the transducer size and decreasing the electric field nonuniformity. Dependence on other sizes of elements appeared to be much weaker. Moreover it was found that extension of backing diameter and addition of dielectric ring around piezocrystal (Fig. 1) reduces nonuniformity of field to a greater extent. In modeling, the dielectric ring was considered to be made from a plastic material.

Model equations and boundary conditions

Piezoelectric was described by equations of electroelasticity in quasi static approximation. [2]: $D_i = \hat{\varepsilon}_{ij}^T E_j + \hat{d}_{ij} \hat{T}_j$, $\hat{T}_i = \hat{c}_{ij}^E \hat{S}_j - \hat{e}_{ki} E_k$, $\partial v_i / \partial t = \rho_0^{-1} \partial T_{ik} / \partial x_k$, $\partial D_i / \partial x_i = 0$, where $\mathbf{E} = -\nabla \varphi$ - electric field strength, φ - electric potential, \mathbf{D} - electric displacement, \hat{S} - strain tensor, \hat{T} - stress tensor, \mathbf{v} - particle velocity, $\hat{\varepsilon}^T$ - permittivity tensor at constant stresses, \hat{c}^E - stiffness matrix at constant electric field, \hat{e} - piezoelectric stress tensor, \hat{d} - piezoelectric strain tensor. The mentioned parameters for the lithium niobate are known. The repeated indices assume summation. Abbreviated notation of tensor indices is applied. For numerical analysis it is convenient to eliminate the strain tensor from the mentioned equations. To do that we differentiate equation for stresses with time. This gives : $\partial \hat{T}_i / \partial t = \hat{c}_{ij}^E \hat{V}_j + \hat{e}_{ki} \partial^2 \varphi / \partial t \partial x_k$, where strain velocities tensor $\hat{V} = \partial \hat{S} / \partial t$ can be expressed in terms of spatial derivatives of vector \mathbf{v} components v_i . Set of the written equations is a basis for the numerical analysis.

Lithium niobate is a member of trigonal system, planar symmetry class (Herman Mogen symbol 3m). Such crystals do not have complete symmetry with respect to rotations around z axis (their lattice grades into itself just at rotations on angles aliquot to 120°), so problem is fundamentally three dimensional and can not be modeled on a personal computer. However, analysis of expressions for material tensors in cylindrical coordinates system shows that all elements that depend on the polar angle are proportional to c_{14} in stiffness matrix and to d_{22} and e_{22} in piezoelectrical tensors. Numerical values of lithium niobate stiffness matrix components are such that c_{14} is much smaller than all other non-zero elements. If it was $c_{14} = 0$, crystal would have been a member of hexagonal system. This system also have planar symmetry class (Herman Mogen symbol 6mm). Crystals of this type have piezoelectric tensors different from those of lithium niobate only by the zeroing of the components d_{22} , e_{22} . From these considerations, in this work lithium niobate was considered in a "hexagonal" approximation. The proof of its validity remains open. Under the made approximations

problem becomes axially symmetric and in cylindrical system of coordinates equations take the following form:

$$\frac{\partial}{\partial t} \begin{pmatrix} T_1 \\ T_2 \\ T_3 \\ T_5 \end{pmatrix} = \begin{pmatrix} c_{11} \frac{\partial v_r}{\partial r} + c_{12} \frac{v_r}{r} + c_{13} \frac{\partial v_z}{\partial z} + e_{31} \frac{\partial}{\partial t} \left(\frac{\partial \varphi}{\partial z} \right) \\ c_{12} \frac{\partial v_r}{\partial r} + c_{11} \frac{v_r}{r} + c_{13} \frac{\partial v_z}{\partial z} + e_{31} \frac{\partial}{\partial t} \left(\frac{\partial \varphi}{\partial z} \right) \\ c_{14} \left(\frac{\partial v_r}{\partial r} - \frac{v_r}{r} \right) \\ c_{44} \left(\frac{\partial v_r}{\partial z} + \frac{\partial v_z}{\partial r} \right) + e_{15} \frac{\partial}{\partial t} \left(\frac{\partial \varphi}{\partial r} \right) \end{pmatrix}, \quad (1)$$

$$\frac{\partial}{\partial t} \begin{pmatrix} v_r \\ v_z \end{pmatrix} = \frac{1}{\rho_0} \begin{pmatrix} \frac{\partial T_1}{\partial r} + \frac{T_1 - T_2}{r} + \frac{\partial T_5}{\partial z} \\ \frac{\partial T_5}{\partial r} + \frac{T_5}{r} + \frac{\partial T_3}{\partial z} \end{pmatrix}, \quad (2)$$

$$\varepsilon_{11}^T \left(\frac{\partial^2 \varphi}{\partial r^2} + \frac{1}{r} \frac{\partial \varphi}{\partial r} \right) + \varepsilon_{33}^T \frac{\partial^2 \varphi}{\partial z^2} = d_{15} \left(\frac{\partial T_5}{\partial r} + \frac{T_5}{r} \right) + d_{31} \left(\frac{\partial T_1}{\partial z} + \frac{\partial T_2}{\partial z} \right) + d_{33} \frac{\partial T_3}{\partial z}, \quad (3)$$

Equations describing motion of copper backing, part of case and water can be obtained from first two equations, Eqs. (1) and (2), by taking there $\hat{e} = 0$ and using the corresponding stiffness matrices. Equation for potential in air is derived from Eq.(3) with $\varepsilon_{11}^T = \varepsilon_{33}^T = \varepsilon_0$, $\hat{d} = 0$.

Interface with air was considered as acoustically pressure release, the side and outer boundaries of the cylindrical layer of water and surface where the case was cut were also considered as pressure release boundaries. At the inner boundaries no special conditions were imposed: instead, the material constants were considered to be dependent of coordinates, i.e. system was considered as an inhomogeneous continuum [3, 5]. In the metal backing, the load electric potential was considered to be given at every time moment, in the casing and radiating surface the potential was equal to zero. On side surfaces of the piezocrystal and dielectric ring condition of electric displacement continuity was imposed. Conditions on axis were obtained from consideration of symmetry: $v_r = 0$, $T_5 \equiv T_{rz} = 0$, $T_6 \equiv T_{r\theta} = 0$, $\partial \varphi / \partial r = 0$.

Method of computing

Equations (1)-(3) were discretized on staggered (by half a step) grids [3,5,6], in doing so various variables and material constants were specified at different points. (Fig. 2). This approach allows to use centered differences for approximation of derivatives. Moreover, terms containing $1/r$ are never computed on the axis itself [5]. In time, variables are separates in the same way: \hat{T} and φ are calculated on the integer steps, \mathbf{v} - on the half integer steps. For approximation of the boundary conditions, one-side differences and, where it was required, fictitious layers of nodes were employed [6]. Equation for potential was solved by successive over relaxation method [4]. Steps in time were done in the following way: from known at time t^p distribution of \hat{T}^p from difference analogue of equation for potential was obtained potential φ^{p+1} at time t^{p+1} , then from equations for stresses were computed \hat{T}^{p+1} . After that field \mathbf{v} was

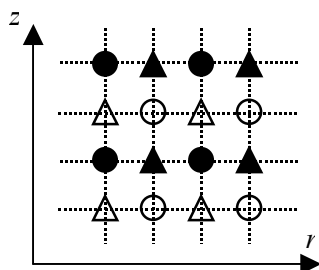


Fig. 2. Relative position of nodes of difference grid for different parameters:

$T_1, T_2, T_3, \hat{c}, \hat{e}$ (○); T_5, \hat{c}, \hat{e} (●);
 v_r, ρ_0 (△); $v_z, \varphi, \rho_0, \hat{\varepsilon}^T, \hat{d}$ (▲).

renewed .

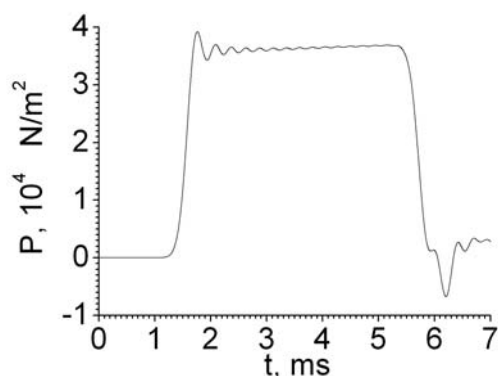


Fig. 3. Waveform on axis, 2 mm from transducer.

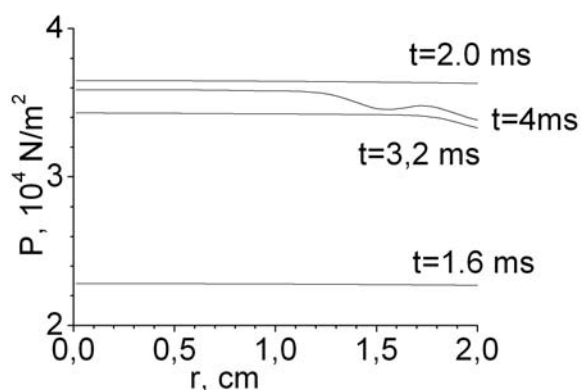


Fig. 4. Radial profiles of pressure, 2 mm from transducer.

Results

On basis of developed algorithm was written program on Matlab language and performed computing for different parameters of system. In Fig. 3 acoustical response on the axis near the transducer is shown. As it is seen, the acoustic wave has a step shape waveform with relatively flat region following the step. In Fig. 4 are shown distributions of instantaneous values of acoustical pressure at different times. Note that in some region near the axis, the wave is plane with a high precision. Such shape of radiated signal is convenient for calibrating hydrophones.

The work is performed under support of grants RFFI 05-02-16987 and Scientific School 4449.2006.2.

REFERENCES

1. F. Lakestani. Etude théorique et expérimentale des transducteurs ultrasonores piézoélectriques fonctionnant dans le domaine du mégahertz. - Thèse doctorat d'état, Institut National des Sciences Appliquées de Lyon, Lyon I, 1984 (in French).
2. N.A. Shulga, A.M. Bolkisev. Vibrations of piezoelectric bodies. - Kiev: Naukova Dumka, 1990 (in Russian).
3. J. Vireux. P-SV wave propagation in heterogeneous media: velocity-stress finite difference method. // Geophysics, vol. 51, 1986, №4.
4. D. Potter. Computational methods in physics. // M.: Mir, 1975 (in Russian).
5. R.O. Cleveland, O.A. Sapozhnikov. Modeling elastic wave propagation in kidney stones with application to shock wave lithotripsy. //JASA v.118, №4, 2005.
6. T. Bohlen, E.H. Saenger, 2006, Accuracy of heterogeneous staggered-grid finite-difference modeling of Rayleigh waves. //manuscript accepted for publication in Geophysics. Available at <http://www.geophysik.uni-kiel.de/~tbohlen/paper.html>